

A LAGRANGIAN APPROACH TO MODELING THE ACCELERATION OF METAL BY EXPLOSIVES

William J. Flis¹

ABSTRACT

Acceleration of metal liners by explosives is modeled by an approach based on Lagrange's principle, which yields not only a final velocity consistent with the widely used Gurney model, but also a velocity history. For explosive slabs and sandwiches, a closed-form velocity history is derived. Cylindrical and spherical charges are also treated but require numerical integration, and example calculations are shown. Finally, applying the approach to the hollow cylindrical charge yields the equations of motion with fewer assumptions than previous models; computed results are compared with hydrocode computations. This work has applications to fragment warheads, shaped charges, and explosive reactive armor.

Introduction

Current models for predicting the projection of metal liners by an explosive are very limited in their applicability. While they may be quite accurate in treating simple configurations, such as spheres and long, uniform cylinders, they can provide only rough estimates of the performance of modern warheads, which are irregularly shaped and often hollow. Most current models fail to provide an acceleration history of the metal, knowledge of which is important for accurately predicting the angle at which the liner is projected (Randers-Pehrson, 1976, and Chou et al., 1981).

The well-known model of Gurney (1943) is limited in that it is essentially an energy method involving only one or two degrees of freedom and can treat only a few simple configurations. It provides the final velocity of a liner, but not its acceleration or velocity history. For modern warheads, Gurney is useful only as an upper bound.

The Gurney model equates the final kinetic energy of the accelerated metal and explosive products gases to the available chemical energy of the explosive, commonly called the Gurney energy E_G , which is taken as a specific property of the explosive. This results in a formula for the final liner velocity V_0 of the form

$$V_0 = \sqrt{2E_G} f(M/C)$$

where the function f of the ratio of metal mass M to explosive charge mass C has a different form for each explosive-metal configuration. For the simple systems shown in Fig. 1, the Gurney velocity is (Thomas, 1944)

$$V_0 = \sqrt{2E_G} \left(\frac{M}{C} + \frac{n}{n+2} \right)^{-1/2} \quad (1)$$

¹ Director of Research, Dyna East Corporation, 3201 Arch Street, Philadelphia, PA.

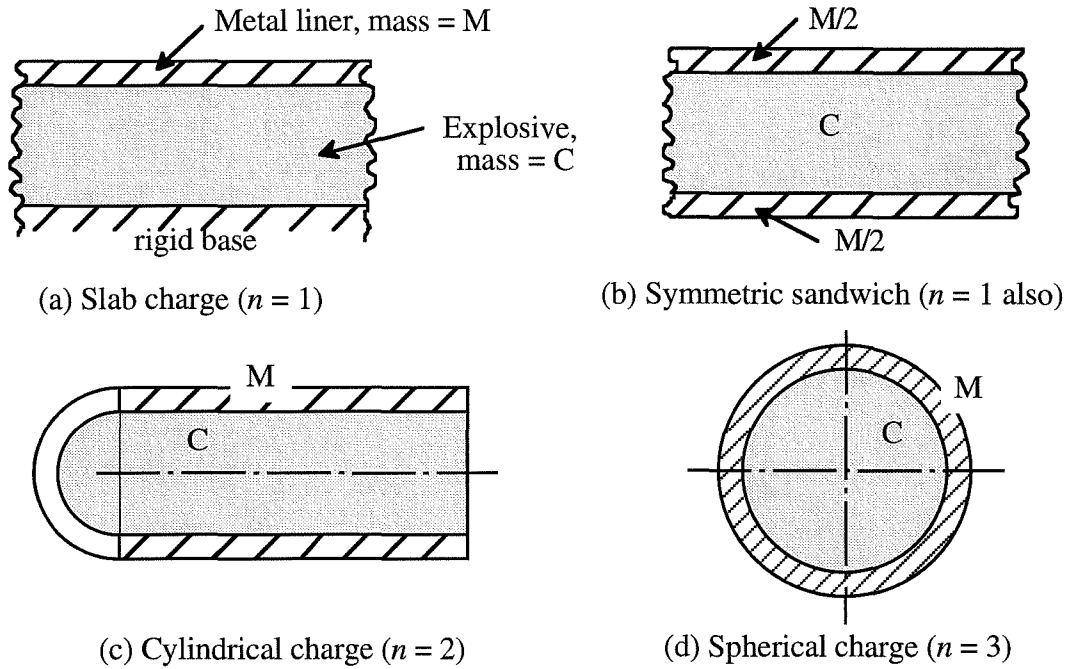


Figure 1. Single-degree-of-freedom explosive-metal systems.

where $n = 1$ for the slab or sandwich, $n = 2$ for the cylinder, and $n = 3$ for the sphere.

The Gurney method has been extended to other configurations, such as cylinders and spheres with rigid cores (Sterne, 1947, 1951), the asymmetric sandwich (Sterne, 1947), the hollow cylinder (Chou et al., 1981, and Chanteret, 1983), and other shapes (Jones, 1965, and Crabtree and Waggener, 1987). Much of this work has been directed toward improving predictions of shaped-charge performance (Chou and Flis, 1986).

Despite these improvements, Gurney still provides only the liner's final velocity, and not its acceleration. A model developed by Henry (1967), however, accounts for the acceleration of the metal by the explosive pressure, which decreases as the explosive expands adiabatically according to the ideal-gas law. The approach is to formulate the equation of motion of the metal, with the explosive pressure P , assumed uniform, as the driving force; e.g., for a slab charge of initial thickness x_0 , an equation is written for the position x of the metal,

$$M \ddot{x} = P = P_0 \left(\frac{v_0}{v}\right)^\gamma = P_0 \left(\frac{x_0}{x}\right)^\gamma$$

where P_0 is the initial pressure of the explosive gas, and each superior dot denotes differentiation with respect to time. A first integral of this equation is

$$\dot{x}^2 = \frac{2 C P_0}{M (\gamma - 1) \rho_0} \left[1 - \left(\frac{x_0}{x}\right)^{\gamma-1} \right]$$

where ρ_0 is the explosive's initial mass density and $C = \rho_0 x_0$ is its mass per unit planar area.

In Henry's model, the initial pressure P_0 is taken as an empirical constant of the explosive in a similar sense as the Gurney energy. However, as Henry recognized, his model is not consistent with Gurney. His final velocity (as $x \rightarrow \infty$) for the systems in Fig. 1 is proportional to $(C/M)^{1/2}$, whereas Gurney's is proportional to $[M/C + n/(n+2)]^{-1/2}$. The reason for this disparity is that, unlike Gurney, Henry does not account for the inertia of the explosive gas.

Jones et al. (1980) addressed the acceleration of planar systems, of which the general case is the asymmetric sandwich, Fig. 2. They enforced conservation of momentum and total energy at all times, with the explosive's internal energy given by the ideal gas law, $E = P\nu/(\gamma - 1)$. To this, they added the equation of motion of one liner, $M_1 d^2x_1/dt^2 = P$, making four equations in x_1 , x_2 , P , and E . However, they imposed no adiabatic or other thermodynamic condition on the explosive. Furthermore, their model is not entirely consistent with Gurney since the explosive's inertia is accounted for only in the conservation equations but not in the plate's equation of motion.

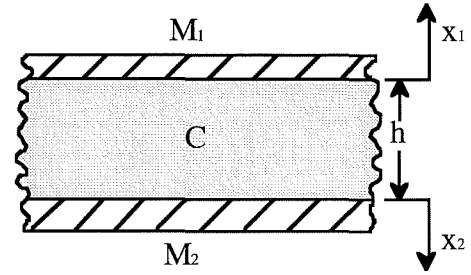


Figure 2. Asymmetric explosive-metal sandwich.

Carleone and Flis (1981, see also Chou et al., 1981) addressed liner acceleration in the hollow cylinder, Fig. 3, which is of interest as an approximation of the cross section of a shaped charge. They recognized that, to apply conservation of momentum to the radial direction, the circumferential component of the explosive pressure must be taken into account and developed a Gurney-like model based on the conservation equations with an empirical formula for the explosive impulse. Previous to this, common practice had been to use the Gurney formula of the asymmetric sandwich to approximate the hollow cylinder. They also developed an expression for the parameters of an exponential velocity history originally proposed by Randers-Pehrson.

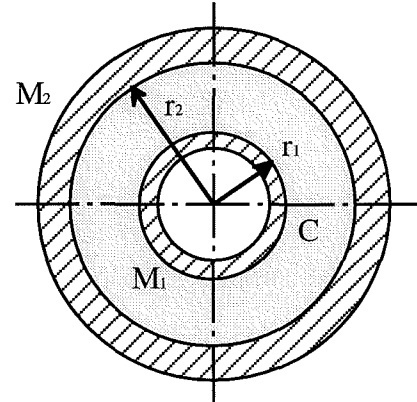


Figure 3. Hollow cylindrical charge.

Hennequin (1983) addressed the hollow cylinder in a similar manner by developing a different empirical formula for the explosive impulse. He modeled the acceleration by requiring conservation of energy at not just the final time but at all times, with the energy of the explosive described by the

ideal-gas adiabat, $E = E_G [1 - (v_0/v)^\gamma]$, or by the JWL equation of state. The models of Chou and Hennequin yielded better agreement with the results of hydrocode computations.

Chanteret (1983) modeled the acceleration of the systems of Fig. 1 as well as the hollow cylinder. His model also requires continual conservation of energy, with the explosive energy given by the ideal-gas adiabat. For the hollow cylinder, he also assumed of the existence within the explosive of a rigid surface that never moves; this allows canceling the explosive impulse from the conservation equations to yield an equation for the radius R_x of the rigid surface,

$$R_x^3 + 3 \left[(R_1 + R_2) \left(R_1 \frac{M_2}{C} + R_2 \frac{M_1}{C} \right) + R_1 R_2 \right] R_x - 3 \left[(R_1 + R_2) R_1 R_2 \left(\frac{2}{3} + \frac{M_1}{C} + \frac{M_2}{C} \right) \right] = 0 \quad (2)$$

(in which some terms accounting for the direction of the detonation wave have been deleted.) After solving for R_x , the energy equation is used to find the final velocities,

$$V_1 = \sqrt{2 E_G} \left(\frac{M_1}{C} \frac{R_2^2 - R_1^2}{R_x^2 - R_1^2} + \frac{1}{6} \frac{3R_1 + R_x}{R_1 + R_x} \right)^{-1/2} \quad \text{and} \quad V_2 = V_1 \frac{R_2 - R_x}{R_x - R_1} \quad (3)$$

Models

This section presents the development of models of several explosive-metal systems following a unified approach based on Lagrange's principle.

Single-Degree-of-Freedom Systems. Henry's model did not account for the inertia of the explosive gas (as did Gurney). However, this may be done through the use of Lagrange's principle. The explosive velocity distribution in the slab charge is assumed to be always linear in the Lagrangian (initial) coordinate X through the explosive, $V_{gas}(X) = x X/x_0$, then the kinetic energy T of the system (per unit planar area) is

$$T = \frac{1}{2} M \dot{x}^2 + \frac{1}{2} \int_{gas} V_{gas}^2 dm_{gas} = \frac{1}{2} M \dot{x}^2 + \frac{1}{2} \int_0^{x_0} \rho_0 \left(\dot{x} \frac{X}{x_0} \right)^2 dX = \left(\frac{1}{2} M + \frac{1}{6} C \right) \dot{x}^2$$

The potential energy U of the system (per unit area) is the internal energy of the explosive gases, which expand adiabatically according to the ideal-gas law,

$$U = - \int P dv = - \int P_0 \left(\frac{v_0}{v} \right)^\gamma dv = \frac{P_0 v_0}{\gamma-1} \left(\frac{v_0}{v} \right)^{\gamma-1} = \frac{P_0 C}{\rho_0 (\gamma-1)} \left(\frac{x_0}{x} \right)^{\gamma-1}$$

Forming the Lagrangian $L = T - U$, and applying Lagrange's equation,

$$\frac{d}{dt} \left(\frac{\partial L}{\partial \dot{x}} \right) - \frac{\partial L}{\partial x} = 0$$

yields the equation of motion,

$$\left(M + \frac{C}{3} \right) \ddot{x} = P_0 \left(\frac{x_0}{x} \right)^\gamma$$

Integration of this equation yields the metal's velocity as a function of its position x ,

$$\dot{x} = \left\{ \frac{2 P_0}{\rho_0 (\gamma-1) \left(\frac{M}{C} + \frac{1}{3} \right)} \left[1 - \left(\frac{x_0}{x} \right)^{\gamma-1} \right] \right\}^{1/2} \quad (4)$$

If we identify P_0 as equal to $\rho_0 (\gamma-1) E_G$, then this is the same result as that of Henry, but forced at large displacement ($x \rightarrow \infty$) to approach the appropriate Gurney velocity,

$$V_0 = \sqrt{2E_G} \left(\frac{M}{C} + \frac{1}{3} \right)^{-1/2}$$

Equation (4) cannot be integrated for general values of γ which varies by explosive from about 2.5 to 3.4. However, for the special case $\gamma=3$ (a good approximation for many explosives), it may be integrated to

$$x = x_0 \sqrt{\left(\frac{t}{\tau} \right)^2 + 1}$$

where time t is reckoned from the beginning of motion and $\tau = x_0/V_0$ is a characteristic period of the system. The velocity history may now be written as

$$\dot{x} = V_0 \frac{t}{\tau} \left[\left(\frac{t}{\tau} \right)^2 + 1 \right]^{-1/2} \quad (5)$$

where the final velocity V_0 is identical to the Gurney velocity for this configuration.

This same approach may be used for any explosive-metal configuration to which the Gurney model is applicable. For the systems in Fig. 1, the Lagrangian is

$$L = \frac{1}{2} \left(M + \frac{n}{n+2} C \right) \dot{x}^2 - \frac{P_0 C}{\rho_0 (\gamma-1)} \left(\frac{x_0}{x} \right)^{n(\gamma-1)}$$

where the explosive mass is $C = \rho_0 x_0$ for $n = 1$, $C = \pi \rho_0 x_0^2$ for $n = 2$, and $C = (4/3) \pi \rho_0 x_0^3$ for $n = 3$, in which x_0 represents the explosive thickness for $n = 1$ and its radius for $n = 2$ or 3.

Application of Lagrange's principle yields the equation of motion,

$$\left(M + \frac{n}{n+2} C\right) \ddot{x} = \frac{n P_0 C}{\rho_0 x_0} \left(\frac{x_0}{x}\right)^{n(\gamma-1)+1}$$

the integral of which yields the velocity as a function of x ,

$$\dot{x} = \left\{ \frac{2 P_0}{\rho_0 (\gamma-1) \left(\frac{M}{C} + \frac{n}{n+2}\right)} \left[1 - \left(\frac{x_0}{x}\right)^{n(\gamma-1)} \right] \right\}^{1/2}$$

If we again identify P_0 as equal to $\rho_0 (\gamma-1) E_G$, then the final velocity is the same as that given by the Gurney model, Eq. (1). This equation cannot be further integrated exactly except for the case of $n (\gamma-1) = 2$, treated above.

Some computed results illustrate the model's behavior. Liner-velocity histories for planar charges ($n = 1$) are plotted for $\gamma = 2.5, 2.7, 3.0$, and 3.4 in Fig. 4(a), with P_0 held fixed. Larger values of γ result in greater rates of acceleration. The differences among these curves are reduced by plotting versus a scaled dimensionless time, t/τ^* , where

$$\tau^* = \frac{2 x_0}{n (\gamma-1) V_0}$$

as shown in Fig. 4(b). This has the effect of making all of the initial slopes (scaled accelerations) equal. The similarity in these scaled curves suggests that the error introduced by the approximation that $\gamma = 3$ can be reduced by substituting τ^* for τ in Eq. (5).

Computed liner-velocity histories for planar, cylindrical, and spherical charges are plotted in Fig. 5 for $\gamma = 3$ again in terms of liner velocity normalized by the final velocity (\dot{x}/V_0) versus scaled dimensionless time (t/τ^*). The differences among these curves demonstrate that the three systems behave differently over time.

Asymmetric Sandwich. The simplest system having two degrees of freedom is the asymmetric sandwich, first analyzed by Sterne (1947), who handled the additional unknown velocity by requiring also conservation of momentum, to yield the formula,

$$V_{G,1} = \sqrt{2E_G} \left[\frac{1+A^3}{3(1+A)} + \frac{M_2}{C} A^2 + \frac{M_1}{C} \right]^{-1/2} \quad \text{where } A = \left(1 + 2\frac{M_1}{C} \right) / \left(1 + 2\frac{M_2}{C} \right)$$

$$V_{G,2} = A V_{G,1} \quad (6)$$

in which the subscripts 1 and 2 refer to the two liners.

To apply the present approach to this system, two Lagrange equations are written. Define x_1 and x_2 as the displacements of the plates, and h as the initial thickness of the explosive layer, as shown in Fig. 2. If the velocity distribution in the explosive is again assumed always linear in the Lagrangian coordinate through the explosive, then the Lagrangian of this system is

$$L = \frac{1}{2} \left[M_1 \dot{x}_1^2 + M_2 \dot{x}_2^2 + \frac{C}{3} (\dot{x}_1^2 - \dot{x}_1 \dot{x}_2 + \dot{x}_2^2) \right] - \frac{P_0 C}{\rho_0 (\gamma-1)} \left(\frac{h}{h+x_1+x_2} \right)^{\gamma-1}$$

Applying Lagrange's principle to each coordinate yields two equations of motion,

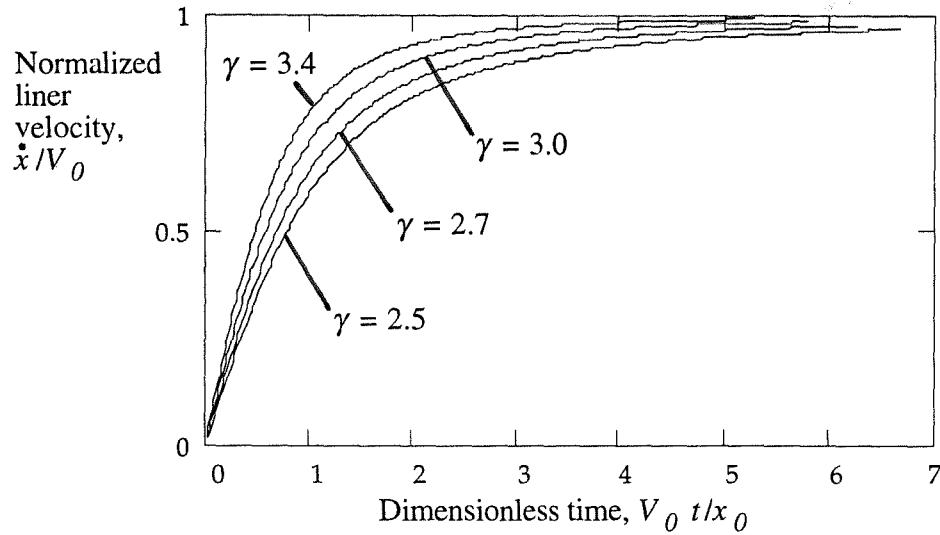
$$\begin{aligned} \left(M_1 + \frac{C}{3}\right) \ddot{x}_1 - \frac{C}{6} \ddot{x}_2 &= P_0 \left(\frac{h}{h+x_1+x_2} \right)^{\gamma} \\ -\frac{C}{6} \ddot{x}_1 + \left(M_2 + \frac{C}{3}\right) \ddot{x}_2 &= P_0 \left(\frac{h}{h+x_1+x_2} \right)^{\gamma} \end{aligned} \quad (7)$$

These equations may be solved by combining them into a single equation in $\chi = x_1 + x_2$; multiplying the first equation by $(M_2 + C/2)$ and the second by $(M_1 + C/2)$ and adding yields

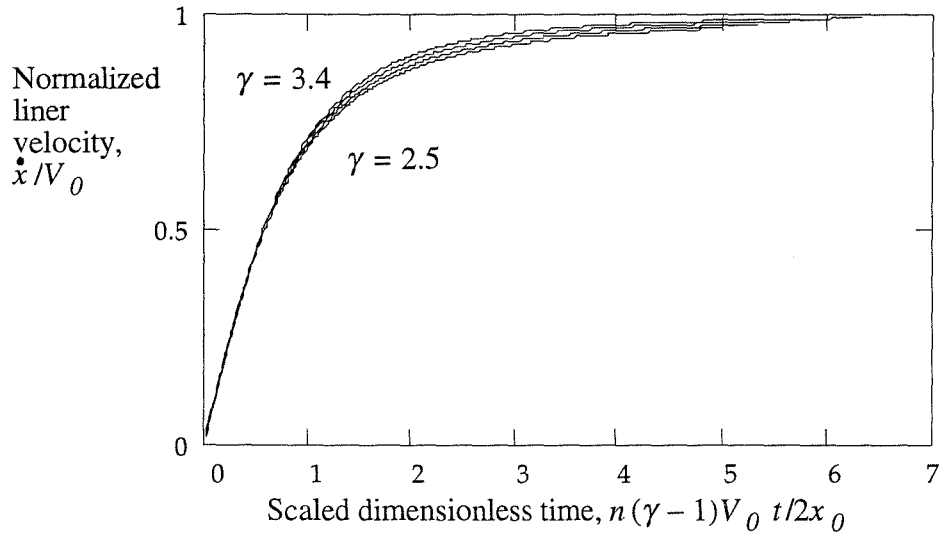
$$\left[M_1 M_2 + \frac{C}{3} (M_1 + M_2) + \frac{C^2}{12} \right] \dot{\chi} = P_0 (M_1 + M_2 + C) \left(\frac{h}{h + \chi} \right)^\gamma$$

A first integral of this equation is

$$\dot{\chi} = \left\{ \frac{2 P_0 C}{\mu \rho_0 (\gamma - 1)} \left[1 - \left(\frac{h}{h + \chi} \right)^{\gamma - 1} \right] \right\}^{1/2} \quad \text{where} \quad \mu = \frac{M_1 M_2 + \frac{C}{3} (M_1 + M_2) + \frac{C^2}{12}}{M_1 + M_2 + C}$$



(a) Normalized velocity vs. dimensionless time



(b) Normalized liner velocity vs. scaled dimensionless time.

Figure 4. Velocity histories predicted by the present model for the planar charge with various values of γ ranging from 2.5 to 3.4.

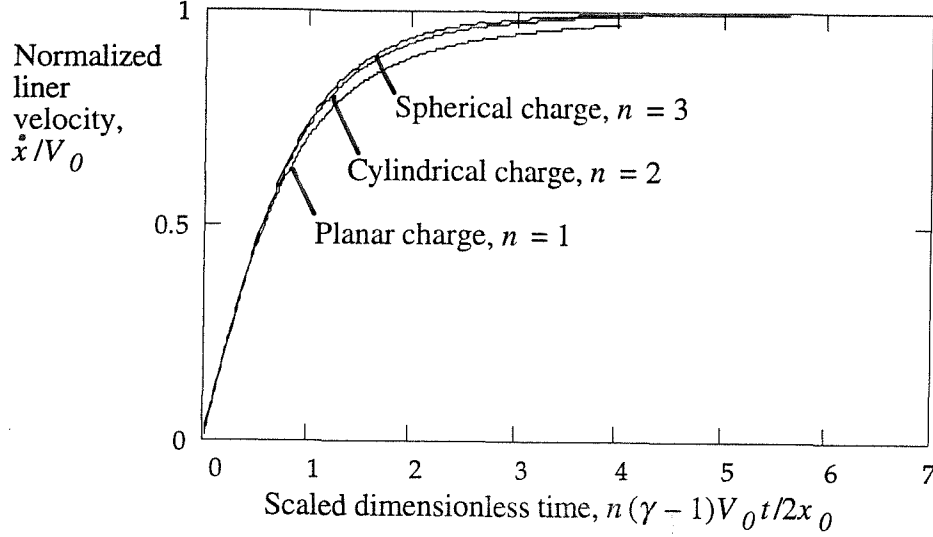


Figure 5. Velocity histories predicted by the present model for the planar charge, cylindrical charge, and spherical charge for $\gamma=3$.

This cannot be further integrated exactly except for the special case $\gamma=3$, which yields

$$\chi = h \left\{ \left[\left(\frac{t}{\tau} \right)^2 + 1 \right]^{1/2} - 1 \right\} \quad (8)$$

where $\tau = \sqrt{h \mu / P_0}$. Now, Eqs. (7) can be decoupled by algebraic manipulation into

$$\frac{M_1 M_2 + C (M_1 + M_2)/3 + C^2/12}{M_2 + C/2} \ddot{x}_1 = P_0 \left[\left(\frac{t}{\tau} \right)^2 + 1 \right]^{-3/2}$$

$$\frac{M_1 M_2 + C (M_1 + M_2)/3 + C^2/12}{M_1 + C/2} \ddot{x}_2 = P_0 \left[\left(\frac{t}{\tau} \right)^2 + 1 \right]^{-3/2}$$

where the quantity $(x_1 + x_2)$ has been replaced by Eq. (8) for χ . These equations may be integrated once to obtain the velocity histories,

$$\dot{x}_1 = V_1 \frac{t}{\tau} \left[\left(\frac{t}{\tau} \right)^2 + 1 \right]^{-1/2} \quad \text{and} \quad \dot{x}_2 = V_2 \frac{t}{\tau} \left[\left(\frac{t}{\tau} \right)^2 + 1 \right]^{-1/2} \quad (9)$$

where V_1 and V_2 are the final velocities, which, if P_0 is again replaced by $E_G \rho_0 (\gamma-1)$, are equal to the Gurney velocities $V_{G,1}$ and $V_{G,2}$ given by Eq. (6). Integrating again yields the displacement histories,

$$x_1 = V_1 \tau \left[\sqrt{\left(\frac{t}{\tau} \right)^2 + 1} - 1 \right] \quad \text{and} \quad x_2 = V_2 \tau \left[\sqrt{\left(\frac{t}{\tau} \right)^2 + 1} - 1 \right]$$

It may be shown that the characteristic time τ for this system is also given by

$$\tau = \frac{h}{V_1 + V_2}$$

Hollow Cylinder. The equations of motion of the hollow cylinder may be derived in a straightforward manner using this approach. Let r_1 and r_2 be the radial coordinates of the interfaces between the explosive and the inner and outer metal liners, with initial values R_1 and R_2 , as shown in Fig. 3. The distribution of velocity in the explosive gas is again assumed linear with respect to the Lagrangian (initial) radial coordinate R ,

$$V_{gas}(R) = \dot{r}_1 + \frac{R - R_1}{R_2 - R_1} (\dot{r}_2 - \dot{r}_1) \quad (10)$$

Then the Lagrangian is

$$L = \frac{1}{2} \left\{ M_1 \dot{r}_1^2 + M_2 \dot{r}_2^2 + \frac{C}{6} \left[\dot{r}_1^2 \frac{3R_1 + R_2}{R_1 + R_2} + \dot{r}_2^2 \frac{R_1 + 3R_2}{R_1 + R_2} + 2\dot{r}_1 \dot{r}_2 \right] \right\} - \frac{P_0 C}{\rho_0 (\gamma - 1)} \left(\frac{R_2^2 - R_1^2}{r_2^2 - r_1^2} \right)^{\gamma - 1}$$

Application of Lagrange's principle to each coordinate r_1 and r_2 yields two equations,

$$\begin{aligned} \left(M_1 + \frac{C}{6} \frac{3R_1 + R_2}{R_1 + R_2} \right) \ddot{r}_1 + \frac{C}{6} \ddot{r}_2 &= -2\pi P_0 \left(\frac{R_2^2 - R_1^2}{r_2^2 - r_1^2} \right)^\gamma r_1 \\ \frac{C}{6} \ddot{r}_1 + \left(M_2 + \frac{C}{6} \frac{R_1 + 3R_2}{R_1 + R_2} \right) \ddot{r}_2 &= 2\pi P_0 \left(\frac{R_2^2 - R_1^2}{r_2^2 - r_1^2} \right)^\gamma r_2 \end{aligned}$$

These coupled equations cannot be solved even partially in closed form, but may be numerically integrated by, for example, the Runge-Kutta method, used in this study.

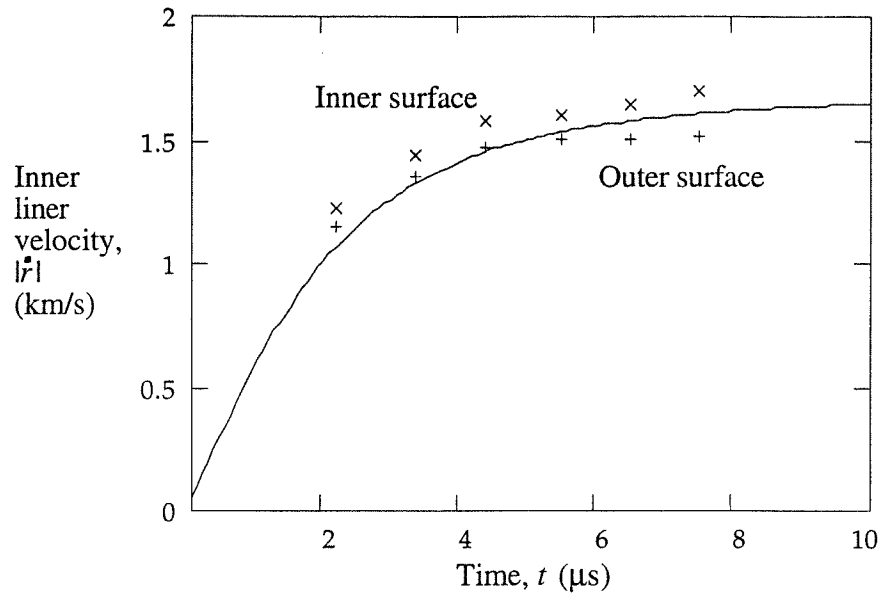
Model predictions are compared with two PISCES code computations reported by Hennequin (1983) in Fig. 6 and 7. The two configurations differ in inner explosive radius, $R_1 = 20$ and 40 mm, but are otherwise the same, having outer radius $R_2 = 50$ mm, with an inner liner of copper and outer liner of steel, each 2-mm thick, with an unspecified explosive modeled by the JWL equation of state. For the model calculations, values of $\gamma = 2.9$, $\rho_0 = 1.8 \text{ Mg/m}^3$, and $\sqrt{(2E_G)} = 2.7 \text{ km/s}$ were chosen, for which $P_0 = 125 \text{ kbars}$. In each figure, velocities of the inner liner are compared in (a), and velocities of the outer liner in (b). For the latter, Hennequin reported velocities of the inner and outer surfaces, which differ because the liner thickens as it moves inwardly.

The present model, like those of Hennequin, Chanteret, and Jones et al., predicts well the final velocities, but provides too low an estimate of the initial acceleration. This is due mainly to the action of the detonation wave, in which the pressure briefly reaches a very high value, about three times the initial pressure P_0 used in these acceleration models.

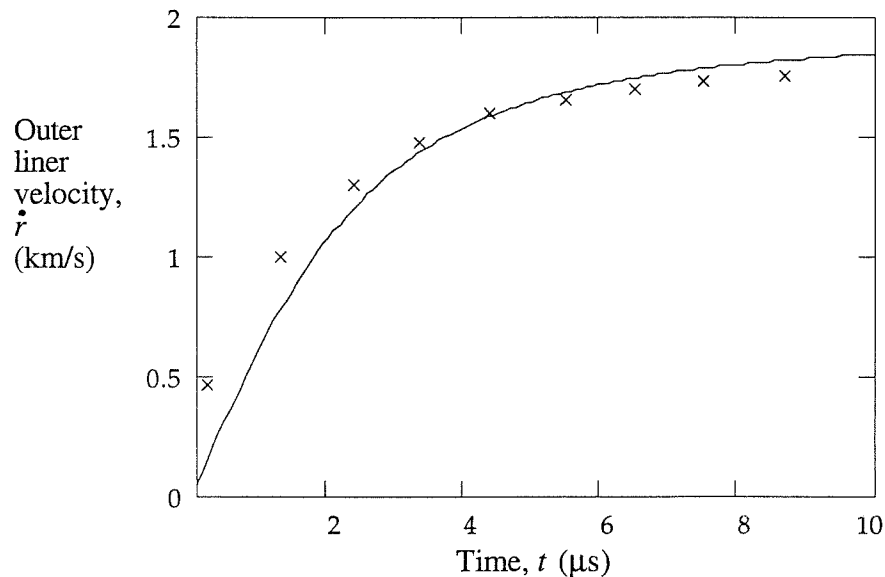
Model predictions were also compared with a series of TEMPS hydrocode computations performed by Carleone and Flis. The ten computed cases had inner radii R_1 of 29 and 40 mm, outer radii R_2 of 50 and 62.5 mm, and various thicknesses h_1 of inner liner; there was no outer liner. The explosive is LX-14, with $\rho_0 = 1.835 \text{ Mg/m}^3$, $\sqrt{(2E_G)} = 3.35 \text{ km/s}$ (which is slightly greater than usually quoted), and $\gamma = 2.841$. Final velocities predicted by the present model, by Chanteret's Eq. (3), and by the Gurney formula for an asymmetric sandwich, Eq. (6), are compared for all cases in Fig. 8 and Table 1. It can be seen in all cases that the present model and Chanteret's model both agree very well with the TEMPS code results. A comparison of the inner-liner velocity history for one particular case is shown in Fig. 9; again, agreement with final velocity is good but initial acceleration is underpredicted by the present model.

An advantage of this model is that a rigid surface is not assumed to exist in the explosive. The model indeed predicts that the point of zero velocity within the explosive moves with respect to the Lagrangian coordinate R . Figure 10(a) shows the predicted velocity distributions in the explosive at several times for the case of Fig. 7. Note that the zero-velocity point moves inward at successive times. This is further shown by Figure 10(b), a plot of the position of the zero-velocity

point over time; the Lagrangian coordinate R of this point, computed by Eq. (10) with $V_{gas} = 0$, decreases from 34.85 mm to about 33.84 mm, whereas Chanteret's model assumes this point is stationary, at $R_x = 34.08$ mm. However, the model-predicted displacement of the zero-velocity point is small, only 3.4% of the explosive thickness ($R_2 - R_1$); thus, it is apparent that the rigid-surface approximation is a good one, as further evidenced by the agreement of Chanteret's predicted velocities in Table 1.

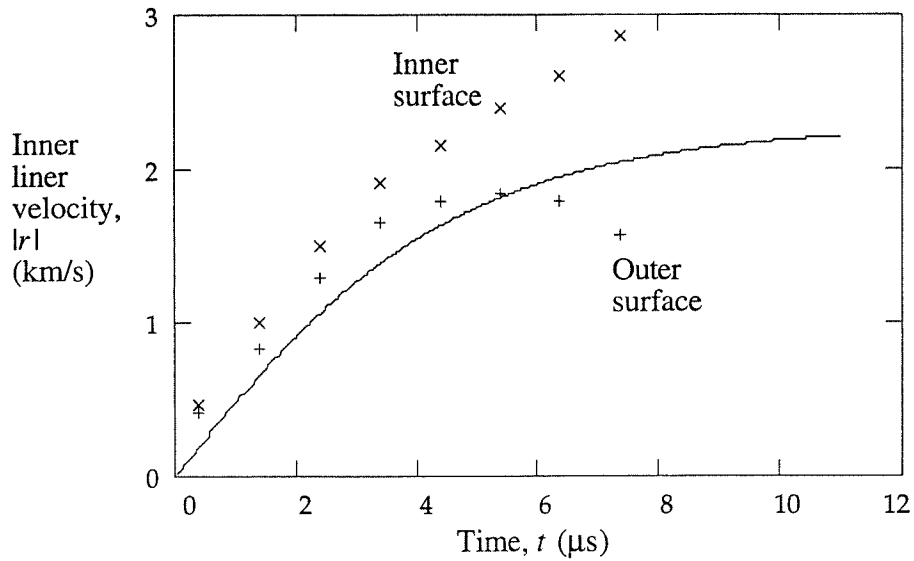


(a) Inner liner

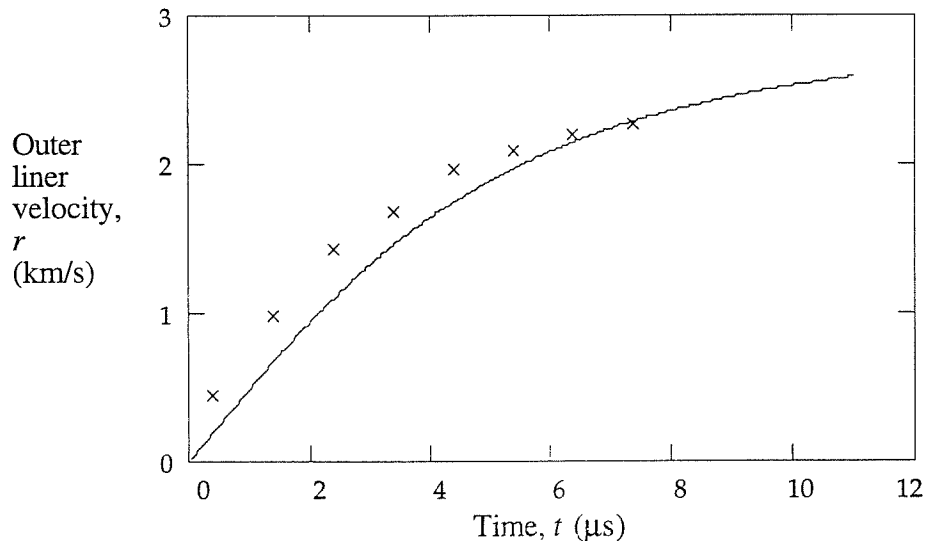


(b) Outer liner

Figure 6. Comparison of liner velocities in a hollow cylindrical charge predicted by the present model (curves) with computations by Hennequin (1983) using the PISCES code (symbols) for $R_1 = 40$ mm, $R_2 = 50$ mm.



(a) Inner liner



(b) Outer liner

Figure 7. Comparison of liner velocities in a hollow cylindrical charge predicted by the present model (curves) with computations by Hennequin using the PISCES code (symbols) for $R_1 = 20$ mm and $R_2 = 50$ mm.

Conclusions

A unified, general approach has been developed for modeling the explosive acceleration of metal liners in several configurations. Models derived using this approach provide not only the liner's final velocity but also its acceleration history. Application to the asymmetric sandwich yields the velocity and displacement history of each liner in closed form. Application to the hollow cylinder allows the use of fewer assumptions than previous models. With some limitations, particularly in predicting the initial acceleration, the model agrees well with the results of two-dimensional hydrocode calculations. This approach may easily be extended to more complex systems having more than two degrees of freedom, such as finite-length hollow cylinders.

Table 1. Comparison of model predictions with the TEMPS hydrocode computations of hollow cylindrical charges by Carleone and Flis (1981).

| R_1 (mm) | R_2 (mm) | h_1 (mm) | Final inner-liner velocity, V_1 (km/s) | | |
|------------|------------|------------|--|-----------|---------------|
| | | | TEMPS | Chanteret | Present model |
| 29 | 50 | 8.0 | 1.230 | 1.25 | 1.38 |
| 29 | 50 | 6.0 | 1.473 | 1.52 | 1.64 |
| 29 | 50 | 2.5 | 2.478 | 2.58 | 2.62 |
| 29 | 50 | 1.2 | 3.483 | 3.62 | 3.50 |
| 29 | 50 | 0.8 | 4.084 | 4.15 | 3.92 |
| 40 | 50 | 4.0 | 1.170 | 1.12 | 1.25 |
| 40 | 50 | 2.5 | 1.626 | 1.57 | 1.73 |
| 40 | 50 | 1.0 | 2.791 | 2.73 | 2.88 |
| 40 | 50 | 0.6 | 3.536 | 3.44 | 3.54 |
| 40 | 62.5 | 7.5 | 1.306 | 1.34 | 1.46 |
| 40 | 62.5 | 2.8 | 2.424 | 2.49 | 2.57 |
| 40 | 62.5 | 1.6 | 3.216 | 3.28 | 3.27 |
| 40 | 62.5 | 1.0 | 3.916 | 3.92 | 3.81 |

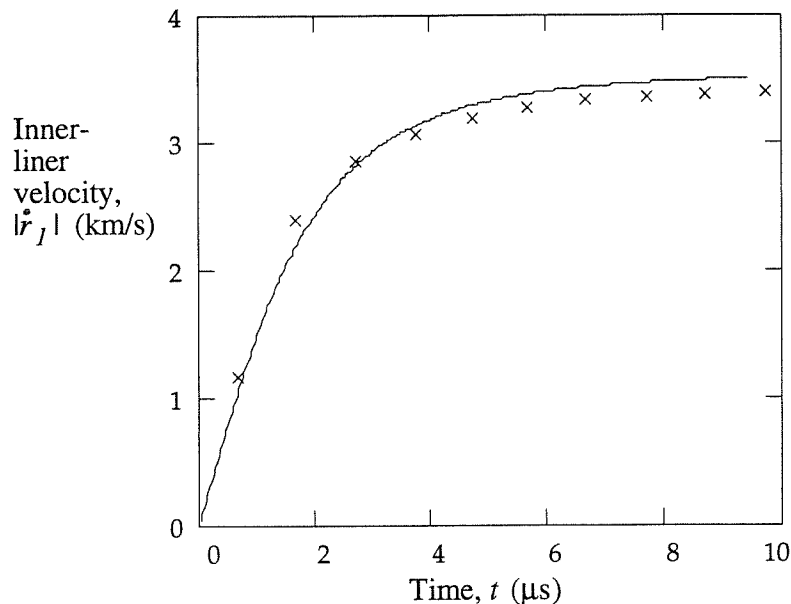


Figure 9. Comparison of the inner-liner velocities in a hollow cylindrical charge, with $R_1 = 29$ mm, $R_2 = 50$ mm, and $h_1 = 1.2$ mm, predicted by the present model (curve) and computed using the TEMPS code (symbols).

Acknowledgments

This work was supported by the Armament Division of Wright Laboratory, Eglin AFB, FL, under Contract FO8630-93-C-0031. The technical guidance of Dr. Joseph C. Foster, Jr., of Wright Laboratory is gratefully acknowledged.

References

Carleone, J., and Flis, W.J., 1982, "Improved Formulas for the Motion of Explosively Driven Liners," Dyna East Corp., Final Report, Contract No. F08635-80-C-0171.

Chanteret, P.Y., 1983, "An Analytical Model for Metal Acceleration by Grazing Detonation," *Proc. 7th Int. Symp. Ballistics*, Shrivenham, UK.

Chou, P.C.; Carleone, J.; Hirsch, E.; Flis, W.J.; and Ciccarelli, R.D., 1981, "Improved Formulas for Velocity, Acceleration and Projection Angle of Explosively Driven Liners," *Proc. 6th Int. Symp. Ballistics*, pp. 262-272, Orlando, FL, 27-29 Oct.

Chou, P.C., and Flis, W.J., 1986, "Recent Developments in Shaped Charge Technology," *Propellants, Explosives, and Pyrotechnics*, Vol. 11, pp. 99-114.

Crabtree, D.K., and Waggener, S.S., 1987, "Gurney-Type Formulas for Estimating Initial Fragment Velocities for Various Warhead Geometries," Naval Surface Weapons Center, Dahlgren, VA, NSWC TR 86-241.

Gurney, R.W., 1943, "The Initial Velocities of Fragments from Bombs, Shells, and Grenades," Ballistic Research Laboratories, Report No. 405.

Hennequin, E.M., 1983, "Analytical Model of Shaped Charge Collapse," *Proc. 7th Inter. Symp. Ballistics*, The Hague, The Netherlands.

Henry, I.G., 1967, "The Gurney Formula and Related Approximations for High-Explosive Deployment of Fragments," Hughes Aircraft Co., Culver City, CA, PUB-189.

Jones, E.E., 1965, "Extension of Gurney Formulas," Honeywell Corp., S5B-4.

Jones, G.E.; Kennedy, J.E.; and Bertholf, L.D., 1980, "Ballistic Calculations of R.W. Gurney," *American Journal of Physics*, V. 48, pp. 264-269.

Randers-Pehrson, G., 1976, "An Improved Equation for Calculating Fragment Projection Angle," *Proc. 2nd Int. Symp. Ballistics*, Daytona Beach, FL, 9-11 March.

Sterne, T.E., 1947, "A Note on the Initial Velocities of Fragments from Warheads," Ballistic Research Laboratories, Report No. 648.

Sterne, T.E., 1951, "The Fragment Velocity of a Spherical Shell Containing an Inert Core," Ballistic Research Laboratories, Report No. 753.